THE JOURNAL OF BIOLOGICAL CHEMISTRY
Vol. 279, No. 50, Issue of December 10, pp. 52406–52413, 2004

Printed in U.S.A.

Critical Role of Calbindin-D28k in Calcium Homeostasis Revealed by Mice Lacking Both Vitamin D Receptor and Calbindin-D28k*

Received for publication, May 19, 2004, and in revised form, September 9, 2004
Published, JBC Papers in Press, September 29, 2004, DOI 10.1074/jbc.M405562200

Wei Zheng‡, Yixia Xie§, Gang Li¶, Juan Kong‡, Jian Q. Feng§, and Yan Chun Li‡‖

From the ‡Department of Medicine, University of Chicago, Chicago, Illinois 60637, the §Department of Oral Biology, School of Dentistry, University of Missouri, Kansas City, Missouri 64108, and the ¶Department of Trauma and Orthopaedic Surgery, School of Medicine, Queen's University Belfast, Musgrave Park Hospital, Belfast BT9 7JB, Northern Ireland United Kingdom

Calbindin (CaBP)-D28k and CaBP-D9k are cytosolic vitamin D-dependent calcium-binding proteins long thought to play an important role in transepithelial calcium transport. However, recent genetic studies suggest that CaBP-D28k is not essential for calcium metabolism. Genetic ablation of this gene in mice leads to no calcemic abnormalities. Genetic inactivation of the vitamin D receptor (VDR) gene leads to hypocalcemia, secondary hyperparathyroidism, rickets, and osteomalacia, accompanied by 90% reduction in renal CaBP-D9k expression but little change in CaBP-D28k. To address whether the role of CaBP-D28k in calcium homeostasis is compensated by CaBP-D9k, we generated VDR/CaBP-D28k double knockout (KO) mice, which expressed no CaBP-D28k and only 10% of CaBP-D9k in the kidney. On a regular diet, the double KO mice were more growth-retarded and 42% smaller in body weight than VDRKO mice and died prematurely at 2.5–3 months of age. Compared with VDRKO mice, the double KO mice had higher urinary calcium excretion and developed more severe secondary hyperparathyroidism and rachitic skeletal phenotype, which were manifested by larger parathyroid glands, higher serum parathyroid hormone levels, much lower bone mineral density, and more distorted growth plate with more osteoid formation in the trabecular region. On high calcium, high lactose diet, blood-ionized calcium levels were normalized in both VDRKO and the double KO mice; however, in contrast to VDRKO mice, the skeletal abnormalities were not completely corrected in the double KO mice. These results directly demonstrate that CaBP-D28k plays a critical role in maintaining calcium homeostasis and skeletal mineralization and suggest that its calcemic role can be mostly compensated by CaBP-D9k.

It is well established that calcium homeostasis is primarily maintained by the vitamin D and parathyroid hormone (PTH)[1] endocrine systems. In this regard, the principal role of vitamin D is to regulate calcium transport in the intestine and kidney. Intestinal and renal distal tubular calcium transfer consists of a passive, concentration gradient-dependent paracellular transport and an active, ATP-dependent transcellular transport (1). The latter is largely regulated by vitamin D and is crucial when calcium supply is low. It is believed that the vitamin D-mediated transcellular calcium transport in the duodenum and renal distal tubules involves three sequential steps: entry, intracellular movement, and extrusion. Influx of luminal calcium into the epithelial cells is propelled by a steep electrochemical gradient across the apical membrane, saturable at high levels of luminal calcium, and mediated by apical calcium channels (2–4). Once in the cytosol, calcium binds to the vitamin D-dependent calcium-binding proteins, calbindins (CaBPs), which ferry calcium from the apical to the basolateral portion of the cell, where the Na^+/Ca^{2+} exchanger and Ca^{2+}-dependent ATPase on the basolateral membrane extrude calcium into extracellular fluids (5–7). It is believed that the apical to basolateral intracellular movement of calcium ions is the rate-limiting step and is highly dependent upon the cellular concentration of CaBPs, which are regulated by 1,25-dihydroxyvitamin D_3, the hormonal form of vitamin D.

CaBPs belong to a family of high affinity calcium-binding proteins that contain the EF-hand structural motif required for calcium binding. Two kinds of CaBPs have been identified: CaBP-D9k, which is mainly expressed in the intestine and kidney, and CaBP-D28k, which is mainly expressed in the kidney and neurons (8). Studies from many laboratories have shown that the expression of both CaBP-D9k and CaBP-D28k is induced by 1,25-dihydroxyvitamin D_3 (9–16). Thus, CaBPs are important vitamin D target genes in the regulation of calcium metabolism.

The co-expression of CaBP-D9k and CaBP-D28k in renal distal tubular cells has long suggested that both are involved in calcium reabsorption. In support of this belief, it has been shown that the development of sustained hypocalcemia in the vitamin D receptor (VDR) knockout (KO) mice is associated with a drastic reduction in renal CaBP-D9k expression (10). However, the role of CaBP-D28k in calcium homeostasis remains controversial. In particular, genetic ablation of the CaBP-D28k gene in mice results in no calcemic abnormalities, with normal serum calcium and phosphate levels (17), and in VDR KO mice, despite their severe hypocalcemia, renal expression of CaBP-D28k is relatively normal (10). These observations may be explained by at least two possibilities. One is that CaBP-D28k is not required for maintaining calcium homeostasis; the other is that the role of CaBP-D28k in calcium metabolism is important but dispensable, and its function can be compensated by CaBP-D9k. To investigate these possibilities, we generated and analyzed mice that lack both VDR and

* This work was supported by National Institutes of Health Grants DK59327 (to Y. C. L.) and AR51587 (to J. Q. F.). The costs of publication of this article were defrayed in part by the payment of page charges. This article must therefore be hereby marked "*advertisement*" in accordance with 18 U.S.C. Section 1734 solely to indicate this fact.

‖ To whom correspondence should be addressed: Dept. of Medicine, University of Chicago, MC 4076, 5841 S. Maryland Ave., Chicago, IL 60637. Tel.: 773-702-2477; Fax: 773-702-5790; E-mail: cyan@medicine.bsd.uchicago.edu.

[1] The abbreviations used are: PTH, parathyroid hormone; CaBP, calbindin; VDR, vitamin D receptor; KO, knockout; GAPDH, glyceraldehyde-3-phosphate dehydrogenase; pQCT, peripheral quantitative computed tomography; BMD, bone mineral density; PBS, phosphate-buffered saline; RT, reverse transcription; WT, wild type.

CaBP-D28k. Our data obtained from these mice provide direct *in vivo* evidence that CaBP-D28k plays a critical role in calcium homeostasis and skeletal mineralization.

MATERIALS AND METHODS

Animals and Breeding Strategy—Generation and characterization of VDR(−/−) mice have been described elsewhere (18). CaBP-D28k(−/−) mice were generated by Airaksinen *et al.* (17) and purchased from The Jackson Laboratories (Bar Harbor, ME). VDR(−/−)/CaBP-D28k(−/−) double KO mice were produced by two breeding steps. First VDR(+/−) mice were bred with CaBP-D28k(−/−) to obtain VDR(+/−)/CaBP-D28k(+/−) mice. Then VDR(+/−)/CaBP-D28k(+/−) × VDR(+/−)/CaBP-D28k(+/−) breeding gave rise to VDR(−/−)/CaBP-D28k(−/−) mice, among other genotypes. Mouse offspring genotyping was carried out by PCR as described previously (17, 18). The animals were housed in a barrier facility on 12-h dark/12-h light cycles. One part of the mouse colonies was fed the regular rodent chow (containing 1% calcium), and another part of the colonies was raised on a high calcium, high lactose diet (HCa-Lac) containing 2% calcium, 1.5% phosphate, and 20% lactose (TD96348, Teklad, Madison, WI) that has been shown to normalize blood-ionized calcium levels in VDR(−/−) mice (19). The body weight and food intake of these mice were determined at 21, 30, 45, and 60 days after birth. To collect urine samples, mice were housed individually in metabolic cages, and urine was collected for 24 h. In all experiments, VDR(−/−)/CaBP-D28k(−/−) mice were analyzed in parallel with age- and gender-matched wild-type (WT), CaBP-D28k(−/−), and VDR(−/−) mice. The use of mice in this study was approved by the Institutional Animal Care and Use Committee of the University of Chicago.

Blood, Serum, and Urinary Parameters—Blood ionized calcium levels were determined using a Model 634 Ca^{2+}/pH analyzer as described before (20). Concentrations of serum phosphorus and urinary calcium, phosphorus, and creatinine were determined by using a Beckman CX5 Autoanalyzer as described previously (20). Serum-intact PTH levels were measured using a commercial enzyme-linked immunosorbent assay kit (Immutopics, San Clements, CA) (20) according to the instructions provided by the manufacturer.

Histological Analysis of Parathyroid Glands and Kidney—The thyroid and parathyroid glands were dissected en bloc with the trachea and fixed overnight in 4% formaldehyde made in PBS (pH 7.2). Kidneys were dissected and immediately fixed with similar procedures. The samples were processed and embedded in paraffin, and serial sections (6 μm) were cut with a Leica 2030 microtome (Leica Microsystems, Nussloch, Germany). The sections were stained with hematoxylin and eosin.

Analysis of Bones—The long bones and vertebrae were dissected after mice were sacrificed and fixed overnight in 4% formaldehyde made in PBS (pH 7.2) after muscles were removed. A high resolution digital x-ray radiographic analysis was conducted using a MX-20 Specimen Radiograph System (Faxitron X-Ray Corp., Wheeling, IL) set at 18 kVp and 5 min. The length of the tibia (from midpoint of tibial plateau to the midpoint of distal tibia) and femur (from the midpoint of the femoral condyles to the tip of the greater trochanter) was measured. The bones (from three to five mice in each genotype) were analyzed by peripheral quantitative computed tomography (pQCT) as well as by histological sectioning described below.

pQCT Analysis—pQCT was carried out using a Stratec XCT 960 M (Norland Medical Systems, Fort Atkinson, WI) as described previously (21). Briefly, femurs and tibiae were analyzed using the manufacturer-supplied software program "XMICE version 1.3" for total bone mineral density, cortical density, and trabecular percentage. A threshold of 1,300 attenuation units was used to differentiate bone from soft tissues, and a threshold of 2,000 was used to differentiate high density cortical bone from low density trabecular bone. Calibration of the pQCT was routinely performed with a set of hydroxyapatite standards. Two femurs or tibiae were placed in the holder each time, and measurements were taken at the diaphyseal midpoint identified in the XCT 960 M scout view.

Bone Histology—For histological analyses, knee joints of distal femur and proximal tibia were fixed in 4% formaldehyde/PBS (pH 7.2), decalcified, and embedded in paraffin by standard histological procedures as described previously (22). Sections were cut and stained with Safranin O (Sigma), followed by counter-staining with hematoxylin, to visualize proteoglycans (23). Bone samples from the other side of the same animals were undecalcified and embedded in methylmethacrylate (Sigma). Five-micron sections were cut and stained with Goldner's trichrome by standard procedures (23), followed by histomorphometric analyses.

RNA Isolation and Northern Blot—Total RNAs were extracted from freshly dissected tissues using TRIzol reagents (Invitrogen). VDR, CaBP-D9k, and CaBP-D28k mRNA transcripts were analyzed by Northern blot as described previously (10). Briefly, total RNAs were separated on 1% formaldehyde-agarose gels and transferred onto nylon membranes. The membranes were hybridized with ^{32}P-labeled cDNA probes. After hybridization the mRNAs were detected by autoradiography and quantified using a PhosphorImager (Amersham Biosciences). The membranes were then stripped and rehybridized with ^{32}P-labeled 36B4 cDNA probe for internal loading control.

Western Blot—The protein level of VDR, CaBP-D9k, and CaBP-D28k was determined by Western blot as described previously (10).

Real Time RT-PCR—Renal expression of TRPV 5 and TRPV6 mRNAs was assessed by real time RT-PCR. Briefly, first strand cDNAs were synthesized from 5 μg of total kidney RNAs in a 50-μl reaction using Moloney murine leukemia virus-reverse transcriptase (Invitrogen) and oligo$(dT)_{12-18}$ as the primer. The cDNAs were then used as the template (5 μl per reaction) for real time PCR amplification. Real time PCR was carried out using a Cepheid Smart Cycler (Cepheid, Sunnyvale, CA) and a SYBR Green PCR Reagent kit (Applied Biosystems, Foster City, CA). The PCR primers for mouse TRPV5 are 5′-CCAGGATAAGATCCGGCTGG-3′ (forward) and 5′-AAAGTAGCGAGAGGCACCAA-3′ (reverse) and for mouse TRPV6 are 5′-GAGGATCCCGATGAGCTGGG-3′ (forward) and 5′-GGGCAGATCCACGTCATAGT-3′ (reverse). These primers were designed according to the cDNA sequences of mouse TRPV5 and TRPV6 as deposited in the GenBank™ data base. GAPDH was used as the internal control for each reaction. GAPDH primers are 5′-CAACTTTGGCATTGTGGAAGG-3′ (forward) and 5′-ACACATTGGGGGTAGGAACAC-3′ (reverse). All primers were tested for their specificity by conventional PCR before being used for the real time PCR quantitative studies. The C_t value for each gene was obtained from the real time PCRs, and the starting amount of each target mRNA was calculated based on a calibration curve and the C_t value. The amount of mRNA for each gene was normalized to GAPDH mRNA and presented as relative values.

Statistical Analysis—Data were presented as the mean ± S.D. and analyzed with Student's *t* test to assess significance. *p* values of 0.05 or lower were considered statistically significant.

RESULTS

A multistep breeding strategy was designed to obtain VDR(−/−)/CaBP-D28k(−/−) mice. Because both VDR(−/−) and CaBP-D28k(−/−) mice were already backcrossed into the C57BL/6 background for at least eight generations, there was little background interference in data interpretation. As shown in Fig. 1, CaBP-D28k(−/−) mice expressed a normal level of VDR and CaBP-D9k, whereas VDR(−/−) mice showed a drastic reduction in CaBP-D9k expression in the kidney at both mRNA and protein levels while maintaining a relatively normal level of CaBP-D28k expression. Exactly as expected, VDR(−/−)/CaBP-D28k(−/−) mice expressed no VDR, no CaBP-D28k, and a very low level of CaBP-D9k as seen in VDR(−/−) mice (Fig. 1, *A* and *B*). Consistent with the previous estimation (10), both VDR(−/−) and double KO mice expressed ~10% of CaBP-D9k in the kidney, relative to the WT levels. Thus, a nearly complete elimination of CaBP proteins was achieved in the kidney of the double KO mice. Both VDR(−/−) and double KO mice maintained about 30% CaBP-D9k in the duodenum, relative to the WT levels (Fig. 1*C*). Therefore, there was no compensatory increase of CaBP-D9k expression in either the kidney or the intestine in CaBP-D28k(−/−) and VDR(−/−)/CaBP-D28k(−/−) mice.

The gross appearance of 2-month old WT, CaBP-D28k(−/−), VDR(−/−), and VDR(−/−)/CaBP-D28k(−/−) mice is shown in Fig. 2. Most double KO mice died at 2.5–3 months of age on regular diet. The premature death was usually accompanied with difficulties in breathing in the last few days of life, but the cause of death was unclear. The body weight of CaBP-D28K(−/−) mice was about the same as WT mice, and VDR(−/−) mice were about 25–30% smaller than WT mice. The double KO mice were the smallest, with a body mass 58% smaller than WT mice and 42% smaller than VDR(−/−) mice at 2 months of age (Fig. 2 and 3*A* and Table I).

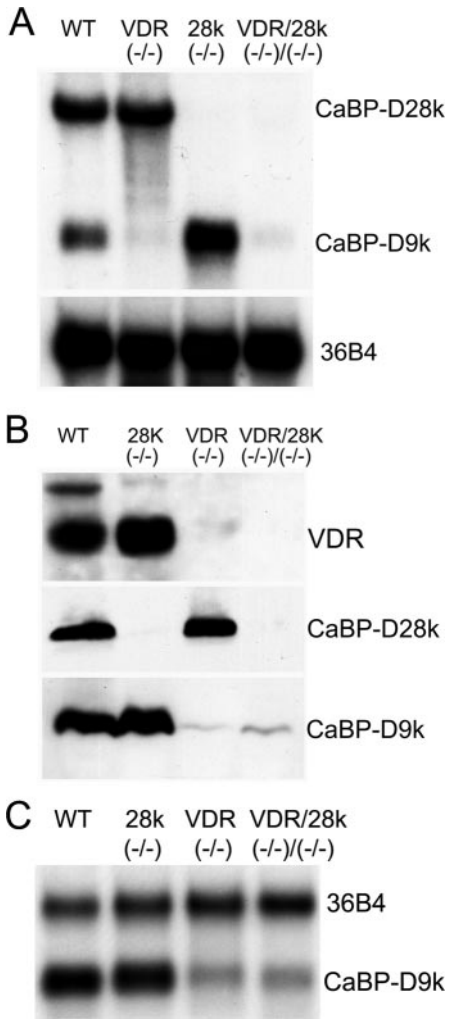

FIG. 1. **Generation of VDR/CaBP-D28k double knockout mice.** *A*, Northern blot analysis of CaBP-D28k and CaBP-D9k expression in the kidney. Total RNAs isolated from the kidney of WT, CaBP-D28k(−/−), VDR(−/−), and VDR(−/−)/CaBP-D28k(−/−) mice were separated on a 1% formaldehyde-agarose gel (20 μg/lane) and probed with ^{32}P-labeled CaBP-D28k, CaBP-D9k, and 36B4 cDNA probes. *B*, Western blot analysis of VDR, CaBP-D28k, and CaBP-D9k expression in the kidney. Kidney lysates obtained from WT, CaBP-D28k(−/−), VDR(−/−), and VDR(−/−)/CaBP-D28k(−/−) mice were separated by PAGE (20 μg/lane) and probed with antibodies against VDR, CaBP-D28k, or CaBP-D9k. *C*, Northern blot analysis of duodenal CaBP-D9k expression in WT, CaBP-D28k(−/−), VDR(−/−), and VDR(−/−)/CaBP-D28k(−/−) mice. The membrane was hybridized with ^{32}P-labeled CaBP-D9k and 36B4 cDNA probes (20 μg/lane).

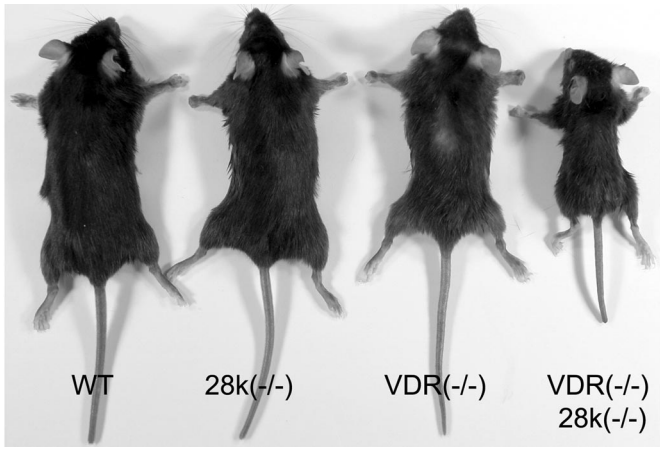

FIG. 2. **The gross appearance of WT, CaBP-D28(−/−), VDR(−/−), and VDR(−/−)/CaBP-D28k(−/−) mice at 2 months of age.** Although VDR(−/−) mice are known to develop alopecia, alopecia usually is not obviously seen until after 3 months of age.

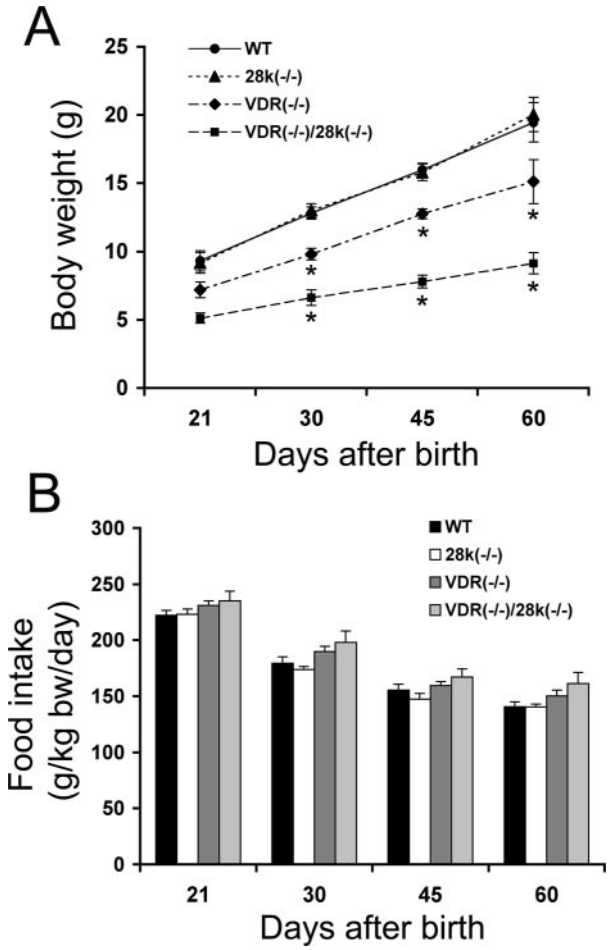

FIG. 3. **Growth curve and food intake of WT, CaBP-D28(−/−), VDR(−/−), and VDR(−/−)/CaBP-D28k(−/−) mice.** *A*, body weight changes between 21 and 60 days after birth. *, $p < 0.001$ *versus* WT mice; $n \geq 5$ in each genotype. *B*, food intake (expressed as per kg of body weight per day) of these four types of mice determined at 21, 30, 45, and 60 days of age. After being normalized to body weight, food intake of these four types of mice is not significantly different.

Fig. 3 shows the growth curve and food intake of WT, CaBP-D28(−/−), VDR(−/−), and VDR(−/−)/CaBP-D28k(−/−) mice within 2 months after birth. The body weight and growth rate of CaBP-D28(−/−) mice were the same as WT mice. Although there was no obvious difference in body size at birth, VDR(−/−) and double KO mice were markedly smaller at weaning (21 days after birth). Even though they were ~25% smaller than WT mice, VDR(−/−) mice were able to maintain a growth rate similar to that of WT mice. In contrast, the double KO mice were more growth-retarded and had a lower growth rate, so the body mass difference between the double KO mice and the WT or VDR(−/−) mice was greater at 2 months than at weaning (Fig. 3*A*). Food intake of WT and CaBP-D28k(−/−) mice was about the same, and food intake of VDR(−/−) and the double KO mice was about 20 and 50% less than that of WT mice, respectively. However, after the food intake was normalized to body weight, there was no significant difference among these four types of mice during this 2-month period (Fig. 3*B*). Food intake decreased with age in all mice.

As shown previously (17, 18), CaBP-D28k(−/−) mice maintained normal levels of blood-ionized calcium and serum phos-

TABLE I
Physiological parameters of 2-month-old WT, CaBP-D28k(−/−), VDR(−/−), and VDR(−/−)/CaBP-D28k(−/−) mice on regular diet

	WT	CaBP-D28k(−/−)	VDR(−/−)	VDR(−/−)/CaBP-D28k(−/−)
Body weight[a] (g)	19.7 ± 2.1 (n = 8)	19.4 ± 1.5 (n = 7)	14.2 ± 1.5[b] (n = 7)	8.3 ± 0.5[b,c] (n = 5)
Blood-ionized Ca^{2+} (mM)	1.32 ± 0.05 (n = 7)	1.29 ± 0.09 (n = 5)	0.88 ± 0.09[b] (n = 5)	0.91 ± 0.11[b] (n = 5)
Serum P_i (mg/dl)	10.5 ± 0.5 (n = 5)	10.8 ± 1.2 (n = 5)	9.2 ± 0.7 (n = 4)	8.9 ± 1.3[d] (n = 5)
Serum-intact PTH (pg/ml)	18.1 ± 12.3 (n = 7)	20.4 ± 9.4 (n = 7)	713.1 ± 282.4[b] (n = 8)	1228.4 ± 750.5[b,c] (n = 6)
Urine Ca^{2+}/creatinine	0.30 ± 0.04 (n = 5)	0.21 ± 0.04 (n = 5)	0.27 ± 0.13 (n = 8)	0.46 ± 0.13[e] (n = 7)
Urine P_i/creatinine	4.16 ± 1.62 (n = 5)	4.38 ± 0.84 (n = 5)	4.59 ± 1.87 (n = 4)	6.29 ± 1.97[d] (n = 4)

[a] Data were from female mice. Similar results were obtained in male mice (not shown).
[b] $p < 0.001$ *versus* WT mice.
[c] $p < 0.01$ *versus* VDR(−/−) mice.
[d] $p < 0.05$ *versus* WT mice.
[e] $p < 0.05$ *versus* VDR(−/−) and WT mice.

phorus and PTH, and VDR(−/−) mice developed hypocalcemia and secondary hyperparathyroidism, with a 30% drop in blood-ionized calcium levels, a 40-fold increase in serum PTH levels, and a modest decrease in serum phosphorus levels at 2 months of age in comparison with WT mice (Table I). These changes were accompanied by a dramatic increase in parathyroid glandular size (Fig. 4*C*), driven by cell proliferation (19). Two-month-old double KO mice had approximately the same low levels of blood-ionized calcium and serum phosphorus, but a much higher serum PTH level (a 68-fold increase over the WT level), as compared with VDR(−/−) mice (Table I). Consistently, the parathyroid gland of the double KO mice showed the largest increase in absolute size (Fig. 4*D*). In fact, the parathyroid hyperplasia was even more dramatic when normalized to body weight, considering that the double KO mice were much smaller than VDR(−/−) mice (Table I and Figs. 2 and 3*A*). Despite the severe hypocalcemia, urinary calcium excretion in VDR(−/−) mice remained approximately the same as seen in WT and CaBP-D28k(−/−) mice (Table I), suggesting renal calcium wasting. Renal calcium wasting was even more severe in the double KO mice, as their urinary calcium concentration was significantly higher than that of VDR(−/−) and WT mice (Table I). There was no significant difference in urinary phosphorus excretion among WT, CaBP-D28k(−/−), and VDR(−/−) mice, but the phosphorus levels in the urine of the double KO mice were significantly higher (Table I). This observation is consistent with our previous studies showing that urinary phosphorus excretion in VDR(−/−) and WT mice is similar (10). The phosphaturia seen in the double KO mice may reflect the more severe secondary hyperparathyroidism in these mice.

The rachitic skeletal phenotype of the double KO mice was clearly more severe than that of VDR(−/−) mice. As shown in Fig. 5, the long bones (tibia and femur) of VDR(−/−) mice were 10–15% shorter than those of WT mice, whereas the long bones of the double KO mice were 10–14% shorter than those of VDR(−/−) mice (Fig. 5*B*). Bone mineralization, as revealed by contact x-ray radiography, was more reduced in the double KO mice than in VDR(−/−) mice, especially in the cortical and trabecular bones (Fig. 5*A*). Consistent with these observations, pQCT analysis demonstrated a remarkable reduction in total, trabecular, and cortical BMD in the long bones of the double KO mice compared with all other groups (Fig. 5*C*). Compared with WT mice, total BMD of VDR(−/−) mice was reduced by 23%, whereas that of double KO mice was reduced by 57% (Fig. 5*C*). The BMD in trabecular and cortical bones was reduced by 14 and 17% in VDR(−/−) mice and by 42 and 53% in the double KO mice, respectively (Fig. 5*C*). Most interestingly, although the bones of CaBP-D28k(−/−) mice appeared normal, a moderate but significant reduction was detected in total and cortical BMD (Fig. 5*C*).

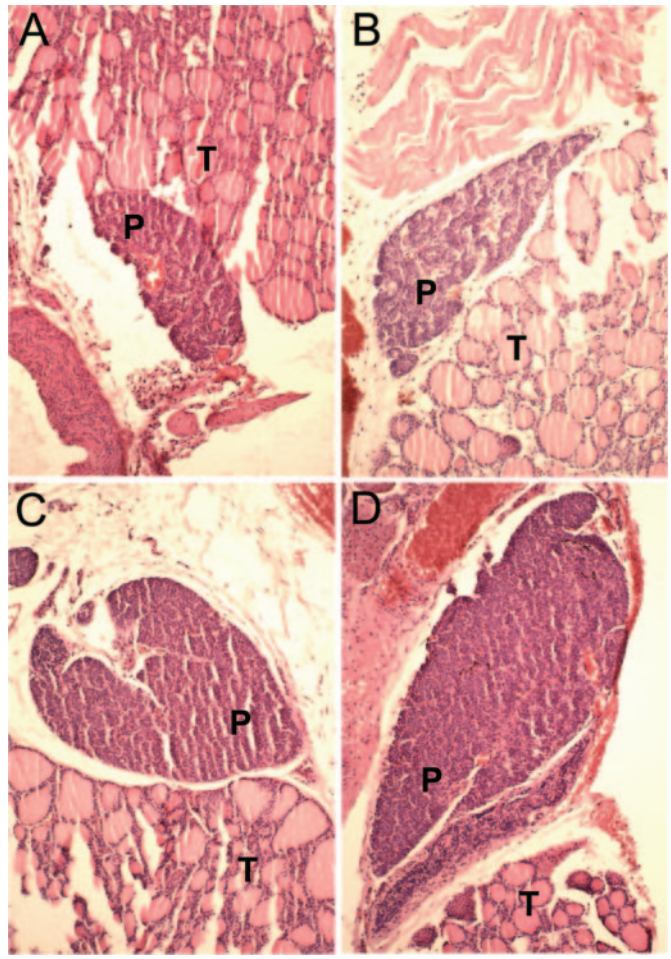

FIG. 4. **Histology of the parathyroid glands.** Sections of the trachea-thyroid-parathyroid region were stained with hematoxylin and eosin. Shown are representative slides of the parathyroid gland from WT (*A*), CaBP-D28(−/−) (*B*), VDR(−/−) (*C*), and VDR(−/−)/CaBP-D28k(−/−) (*D*) mice at 2 months of age. *T*, thyroid gland; *P*, parathyroid gland.

Histological analyses revealed remarkable rachitic bone abnormalities in both VDR(−/−) and double KO mice. These were characterized by a highly irregular and disorganized growth plate, a marked expansion of the hypertropic chondrocyte zone, and a dramatic increase in osteoid content in trabecular and

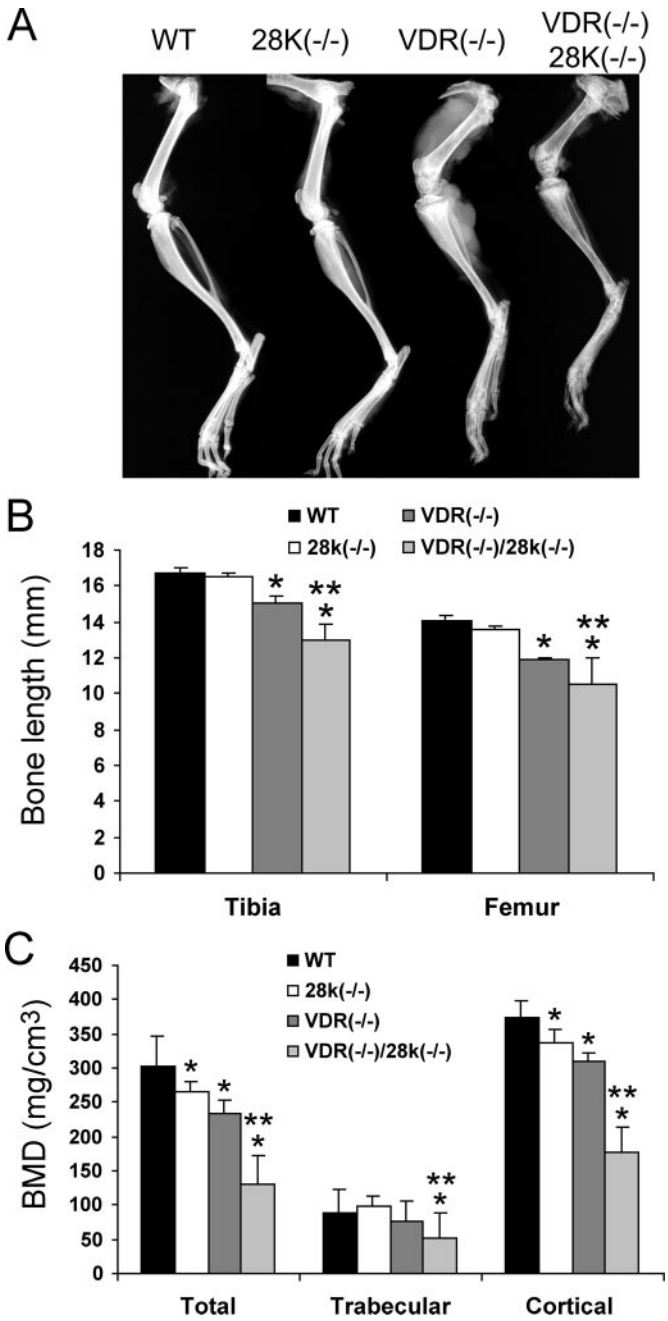

FIG. 5. **Bone data from WT, CaBP-D28(−/−), VDR(−/−), and VDR(−/−)/CaBP-D28k(−/−) mice at 2 months of age.** *A*, contact x-ray radiography of the long bones. *B*, the length of tibia and femur (mm). *, $p < 0.05$ *versus* WT mice; **, $p < 0.01$ *versus* VDR(−/−) mice. $n = 4$. *C*, total, trabecular and cortical bone mineral density (*BMD*) quantified by pQCT. *, $p < 0.05$ *versus* WT mice; **, $p < 0.001$ *versus* VDR(−/−) mice; $n = 4$.

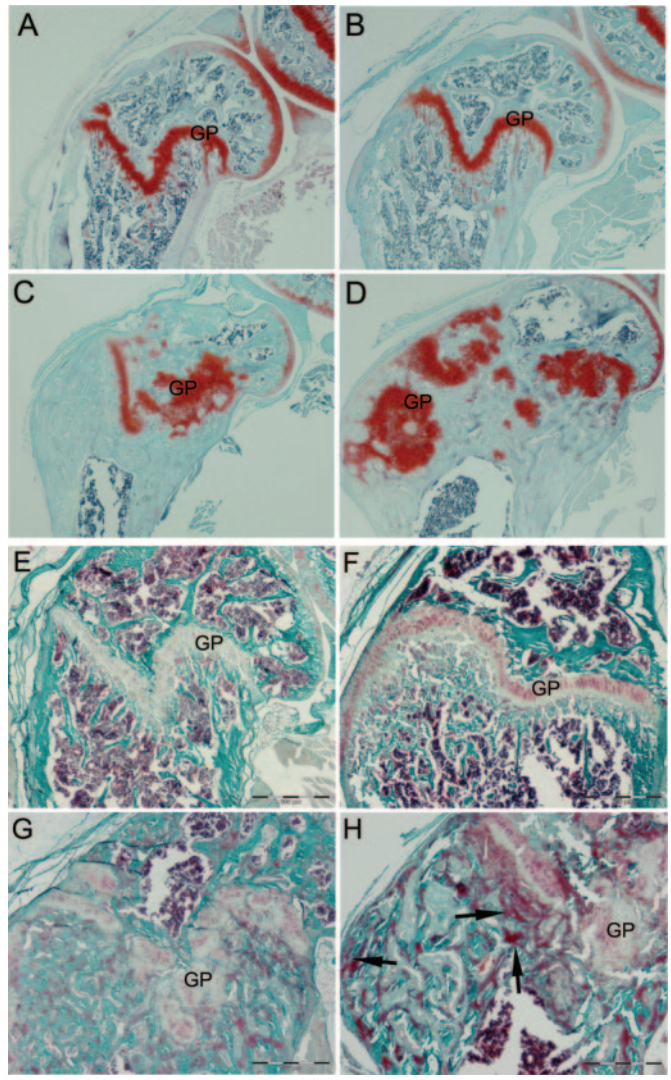

FIG. 6. **Histological analysis of the bones from 2-month-old WT (*A* and *E*), CaBP-D28(−/−) (*B* and *F*), VDR(−/−) (*C* and *G*), and VDR(−/−)/CaBP-D28k(−/−) (*D* and *H*) mice on a regular diet.** *A–D*, Safranin O staining of the tibia. Proteoglycans are stained *bright red*. The bones were decalcified before staining. Magnification, ×20. *E–H*, Goldner's trichrome staining of the tibia. The bones were cut undecalcified before staining. Mineralized matrix is stained *green* and non-mineralized matrix stained *dark pink*. Magnification, ×40. *GP*, growth plate. Note the highly deformed growth plate (*D*) and the large accumulation of unmineralized matrix (*H*, indicated by *arrows*) in the double KO mice.

cortical bones (Fig. 6). Large clusters of immature, poorly mineralized woven bones were present in VDR(−/−) and the double KO mice, indicating impaired mineralization of the newly formed bones (Fig. 6, *G* and *H*). Compared with VDR(−/−) mice, however, the double KO mice displayed much more severe skeletal abnormalities. The growth plate was more deformed, and the chondrocyte columns appeared more discontinuous and disoriented (compared Fig. 6, *C* and *D*); Goldner trichrome staining showed much more unmineralized osteoid accumulation (pink staining) throughout the trabecular and metaphysis regions in the double KO mice (compare Fig. 6, *G* and *H*).

On the high calcium, high lactose diet, the body weight, blood-ionized calcium, and serum phosphorus levels of both VDR(−/−) and double KO mice were in the normal range (Table II), and no death was seen in the double KO mice 3–4 months after birth. Serum PTH levels in these mice were greatly improved but still relatively higher (Table II), apparently because of the lack of VDR-mediated vitamin D suppression of PTH production (24, 25). As expected, consumption of the calcium-enriched diet led to a greater amount of calcium excreted into the urine in all four types of mice than they were on the regular diet (compare urinary calcium levels in Table I and II); however, most strikingly, urinary calcium excretion in VDR(−/−) and double KO mice was 2–3 times higher than that of WT and CaBP-D28(−/−) mice fed the same HCa-Lac diet (Table II), confirming the defect in calcium reabsorption in VDR(−/−) and double KO mice. There was no significant difference in urinary calcium levels between VDR(−/−) and double KO mice. Urinary phosphorus levels among these four types of mice were similar, but generally lower than the levels when

TABLE II
Physiological parameters of 2-month old WT, CaBP-D28k(−/−), VDR(−/−), and VDR(−/−)/CaBP-D28k(−/−) mice raised on high calcium, high lactose diet

	WT[a]	CaBP-D28k(−/−)[a]	VDR(−/−)[a]	VDR(−/−)/CaBP-D28k(−/−)[a]
Body weight (g)	17.1 ± 2.2	18.1 ± 2.3	19.4 ± 2.6	16.9 ± 3.5
Blood-ionized Ca^{2+} (mM)	1.41 ± 0.07	1.36 ± 0.08	1.32 ± 0.07	1.29 ± 0.07
Serum P_i (mg/dl)	10.5 ± 0.6	9.4 ± 0.6	10.6 ± 1.9	10.3 ± 2.5
Serum-intact PTH (pg/ml)	15.2 ± 1.7	13.6 ± 6.5	247.5 ± 117.1[b]	207.1 ± 101.2[b]
Urine Ca^{2+}/creatinine	2.51 ± 1.32	1.87 ± 0.83	6.57 ± 1.25[c]	5.64 ± 2.12[c]
Urine P_i/creatinine	1.7 ± 0.7	1.71 ± 0.69	2.05 ± 0.87	1.83 ± 0.41

[a] $n \geq 4$.
[b] $p < 0.01$ *versus* WT mice.
[c] $p < 0.05$ *versus* WT mice.

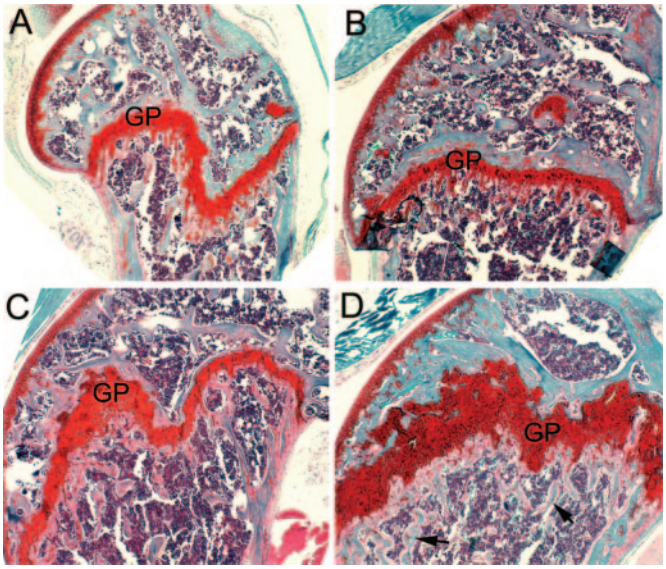

FIG. 7. **Safranin O staining of the tibia from 2-month-old WT (*A*), CaBP-D28(−/−) (*B*), VDR(−/−) (*C*), and VDR(−/−)/CaBP-D28k(−/−) (*D*) mice raised on the high calcium, high lactose diet.** Note the still expanded growth plate in the double KO mice (*D*). *GP*, red-stained growth plate. *Arrows* indicate poorly mineralized trabecular bones.

the mice were on the regular diet (compare Table I and II). In connection with these improvements, the bone of VDR(−/−) mice was grossly normal (Fig. 7*C*). Most interestingly, expanded growth plate chondrocyte columns remained in the double KO mice (Fig. 7*D*), consistent with more a more negative calcium balance in these mice.

The epithelial calcium channels, TRPV5 and TRPV6, play a key role in transepithelial calcium transport in renal tubules, as they facilitate and regulate calcium entry into the cell across the apical membrane (26, 27). To assess the effect of inactivation of CaBP-D28k, VDR, or both on these calcium channels and to investigate whether the decrease in renal calcium reabsorption is associated with a decrease in TRPV5 and TRPV6 expression, the mRNA levels of these two genes in the kidneys of WT, CaBP-D28(−/−), VDR(−/−), and VDR(−/−)/CaBP-D28k(−/−) mice were quantified by real time RT-PCR. As shown in Fig. 8, on regular diet, CaBP-D28k ablation had little effect on TRPV5 or TRPV6 expression, whereas VDR inactivation significantly reduced both TRPV5 and TRPV6 expression by 46 and 40%, respectively (Fig. 8, *A* and *B*). Inactivation of both VDR and CaBP-D28k had no additive effects on the expression of these two genes, because the levels of both TRPV5 and TRPV6 were not significantly different between VDR(−/−) and the double KO mice (Fig. 8, *A* and *B*). On the HCa-Lac diet, the expression of these two genes was generally lower in all mice than when they were on the regular diet, consistent with the higher urinary calcium excretion (Table II). The relative expression levels in VDR(−/−) and double KO mice remained lower than in WT and CaBP-D28k(−/−) mice (Fig. 8, *A* and *B*).

DISCUSSION

One important determinant of calcium balance is renal handling of calcium. In normal adult animals, a major portion (95%) of filtrated calcium is reabsorbed, and only a small fraction (2–5%), which is approximately equal to the amount of calcium absorbed from the intestine, is excreted into the urine to maintain a calcium balance. In the nephron, the majority of filtered calcium is reabsorbed in the proximal convoluted tubules and the loop of Henle by the paracellular process. In the distal convoluted tubule, calcium is reabsorbed through the ATP-dependent transcellular process, which largely determines the amount of calcium excreted into the urine (28, 29). Because both CaBP-D9k and CaBP-D28k are co-expressed in the distal tubule, have potent calcium-binding capacity, and are regulated by vitamin D, they are long thought to be critically involved in vitamin D-regulated calcium reabsorption in the kidney (8). Consistent with this notion, a correlation between 90% reduction in renal CaBP-D9k expression and renal calcium wasting has been observed in VDR(−/−) mice, suggesting that CaBP-D9k indeed plays a key role in calcium reabsorption (10, 30).

However, the role of CaBP-D28k in calcium metabolism is less clear. In contrast to CaBP-D9k, renal CaBP-D28k expression is relatively normal in VDR(−/−) mice, inappropriate for the severe hypocalcemia and hypercalciuria seen in these mice (10). Renal CaBP-D9k, but not CaBP-D28k, responds to changes in dietary calcium content; CaBP-D9k levels increases when WT mice are fed a low calcium (0.02%) diet and decreases on a high calcium (2%) diet, whereas CaBP-D28k levels remain relatively unchanged under these two dietary conditions (31).[2] More surprisingly, mice lacking CaBP-D28k develop problems in the nervous system but no abnormalities in systemic calcium metabolism, with normal serum calcium, phosphate, and PTH levels (17). The bone phenotype, presumably normal, was not investigated when the KO mice were first reported. More recent studies reported that CaBP-D28k(−/−) mice fed a 1% calcium diet had higher urinary calcium excretion and a lower bone turnover rate than WT mice, even though their serum calcium levels and intestinal CaBP-D9k expression were normal (31, 32). In theory, to maintain a calcium balance, these mutant mice need to have increased intestinal calcium absorption and/or higher bone turnover, which is contradictory to the normal intestinal CaBP-D9k levels and lower bone turnover seen in these mice. Therefore, the mechanism underlying the hypercalciuria remains to be explored.

In the present study we systematically examined CaBP-D28k(−/−) mice fed a regular (1%) or high (2%) calcium diet. Our data show that these mutant mice have normal body weight, normal levels of serum-ionized calcium, phosphorus,

[2] M. J. G. Bolt and Y. C. Li, unpublished data.

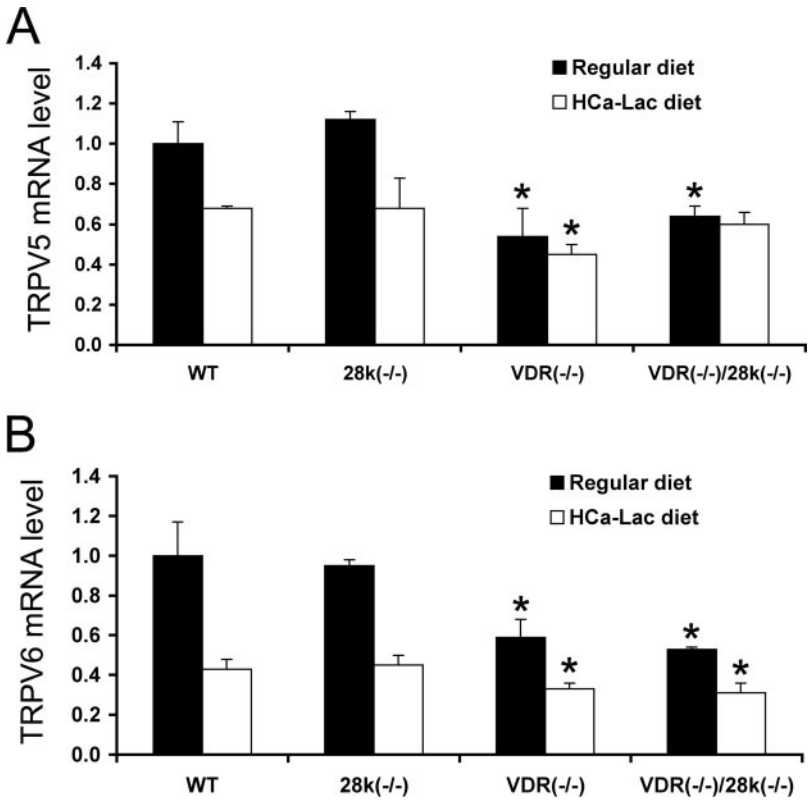

FIG. 8. **Expression of epithelial calcium channels in the kidney.** Kidney total RNAs were isolated from WT, CaBP-D28k(−/−), VDR(−/−), and VDR(−/−)/CaBP-D28k(−/−) mice raised on regular diet or on the high calcium, high lactose diet. Levels of TRPV5 (*A*) and TPRV6 (*B*) mRNA transcripts in the kidneys were quantified by real time RT-PCR. The mRNA levels of these genes were normalized with GAPDH mRNA and presented as the ratio. *, $p < 0.05$ *versus* WT mice on the same diet; $n = 4$. There is no significant difference between VDR(−/−) and VDR(−/−)/CaBP-D28k(−/−) mice on either regular or high calcium, high lactose diet.

and PTH, and normal levels of urinary calcium and phosphorus under both dietary conditions. Bone histological structure appears normal, except for a modest decrease in BMD. The modest decrease in BMD might reflect a long term effect of subtle calcium wasting that cannot be accurately measured by our current method or a direct effect of CaBP-D28k inactivation on osteoblasts, which express CaBP-D28k (33, 34). We do not have an explanation for the discrepancy between our observations and previously reported urinary calcium data described above, other than noticing the difference in analytic methods (*e.g.* automatic analyzer *versus* colorimetric assay kits) and animal age (*e.g.* 2-months *versus* 4 weeks old).

A definitive conclusion about the role of CaBP-D28k in calcium metabolism comes from the studies of the double KO mice. Here we took advantage of the fact that VDR(−/−) mice lost 90% of renal CaBP-D9k expression and generated double KO mice that express no CaBP-D28k and only 10% CaBP-D9k in the kidney. We reasoned that if CaBP-D28k is compensated by CaBP-D9k in CaBP-D28k(−/−) mice, then CaBP-D9k will not be able to compensate for CaBP-D28k in the double KO mice because of its dramatic reduction in the kidney. Therefore, the double KO mice should provide an animal model in which the role of CaBP-D28k can be assessed with little interference from CaBP-D9k. As expected, the double KO mice have much higher urinary calcium wasting than VDR(−/−) mice on regular diet, reflecting the loss of transcellular calcium transport mediated by CaBP-D9k and CaBP-D28k and the loss of CaBP-D9k compensation for CaBP-D28k. Higher calcium wasting in the double KO mice leads to more severe hyperparathyroidism, which then causes more phosphate excretion and bone resorption. Therefore, compared with VDR(−/−) mice, the more severe parathyroid and skeletal abnormalities seen in the double KO mice, manifested by higher serum PTH, more severe parathyroid hyperplasia, lower BMD, and more osteoid accumulation, are a consequence of higher chronic calcium wasting in these mice. Under the high calcium dietary condition, blood-ionized calcium levels can be normalized in both VDR(−/−) and double KO mice because of ample calcium supply from the food. Urinary calcium excretion in these two types of mice is dramatically increased, consistent with impaired reabsorption, but the difference between them disappears (Table II). This may reflect the fact that the long term calcium oversupply has overwhelmed the ultrafiltered calcium load in both VDR(−/−) and double KO mice, so that the unreabsorbed fraction become indistinguishable between these mice. Even though normal blood-ionized calcium levels are maintained with a high calcium supply and the double KO mice survive well, in contrast to VDR(−/−) mice, their rachitic skeletal phenotype cannot be completely rescued, confirming that the double KO mice still suffer a negative calcium balance. These data provide convincing *in vivo* evidence that CaBP-D28k does play a critical role in calcium metabolism. Therefore, both CaBP-D9k and CaBP-28k are important for renal calcium handling. Other data from recent studies of 25-hydroxyvitamin D_3 1α-hydroxylase knockout mice are consistent with this conclusion (5).

Although the double KO mice were born alive and showed no obvious developmental abnormalities, they failed to thrive and usually survived for only 2.5–3 months after birth on the regular diet. The cause of premature death is unclear at this time. Histological examination of the kidney shows no obvious renal abnormalities or damages in the double KO mice, and their serum creatinine and blood urea nitrogen levels are in the normal ranges (creatinine, 0.56 ± 0.32 in WT *versus* 0.47 ± 0.13 mg/dl in double KO; and blood urea nitrogen, 22.6 ± 4.2 in WT *versus* 31.5 ± 4.4 mg/dl in double KO). Thus, renal failure as the cause of failure to thrive and early death can largely be excluded. Impaired insulin secretion with reduced insulin mRNA expression has been reported in VDR(−/−) mice (35), whereas a greater stimulation of insulin secretion by KCl has been reported in CaBP-D28k(−/−) mice (36). We found that pancreatic insulin mRNA levels in the double KO mice are normal in comparison with WT mice (data not shown), which rules out insulin as the cause. Although impaired food intake may potentially be a factor for severe growth retardation, food

intake of the double KO mice is appropriate for their body weight. We speculate that one possible cause of early death for the double KO mice is an ultimate respiratory arrest caused by a collapse of the highly de-mineralized rib cage, because these mice show signs of difficult breathing in the last few days before death, and x-ray radiography shows that the rib cage from the double KO mice appears more de-mineralized than that of VDR(−/−) mice (data not shown). Another more likely possibility is that, because of uncontrollable calcium wasting, the body eventually lost the ability to maintain a minimal blood calcium level required for survival. Once the blood calcium level drops below a critical threshold, the mice die. This possibility may explain why the double KO mice have the same blood-ionized calcium levels as VDR(−/−) mice at 2 months of age, because that may be the minimal calcium concentration required for survival. The double KO mice maintain the minimal calcium concentration at a higher expense of the skeleton than VDR(−/−) mice because of more severe chronic calcium wasting in the kidney, leading to more severe bone abnormalities. This is compounded by the more severe secondary hyperparathyroidism developed in the double KO mice, which stimulates more bone resorption to counter the calcium wasting. Thus, severe chronic calcium wasting may be the major contributing factor for the failure to thrive and premature death in the double KO mice.

Since the cloning of the apical calcium channels from vitamin D-responsive epithelia (4, 37), TRPV5 (or ECaC1, CaT2) and TRPV6 (or CaT1, ECaC2) have been shown to be crucial for transepithelial calcium transport and calcium handling (26, 27). Previous studies on the effect of dietary calcium or vitamin D on expression of these calcium channels in the kidney have presented somewhat conflicting results. Some studies show that these genes are regulated by calcium but not 1,25-dihydroxyvitmain D_3 in mice lacking VDR (38), whereas others show that they are modulated by both calcium and 1,25-dihydroxyvitmain D_3 in WT mice (39) and in mice lacking 1α-hydoxylase (5). A previous report also shows that levels of TRPV5 are not altered in CaBP-D28k(−/−) mice (32). Here we demonstrate that expression of both TRPV5 and TRPV6 is not changed in CaBP-D28k(−/−) mice but down-regulated by about the same magnitude in both VDR(−/−) and double KO mice. High calcium diet suppresses both TRPV5 and TRPV6 in the four types of mice, but their expression in VDR(−/−) and double KO mice remains lower. These results confirm that the apical calcium channels are regulated by both calcium and vitamin D, and ablation of CaBP-D28k has no stimulatory effects on both channels.

In summary, analyses of the mice lacking both VDR and CaBP-D28k demonstrate that CaBP-D28k does play a critical role in calcium metabolism, and CaBP-D28k-mediated transcellular calcium transport in the distal tubule of the kidney is important for calcium reabsorption. It is possible that the role of CaBP-D28k in the kidney can be mostly compensated by CaBP-D9k, as seen in CaBP-D28k(−/−) mice, which express a normal level of CaBP-D9k and develop little calcemic abnormalities. However, the fact that CaBP-D28k(−/−) mice still show a modest decrease in BMD suggests that CaBP-D9k cannot completely compensate for the function lost with CaBP-D28k ablation. CaBP-D9k, on the other hand, cannot be compensated by CaBP-D28k, as shown in VDR(−/−) mice, which express 10% of CaBP-D9k and a relatively normal level of CaBP-D28k in the kidney but develop hypocalcemia and rickets (10). In this regard, it will be very interesting to analyze the phenotype of CaBP-D9k(−/−) mice, but generation of these mutant mice has not been reported yet. In theory, a more definitive conclusion about the role of CaBP-D9k and CaBP-D28k may come from studies of CaBP-D9k(−/−) and CaBP-D9k(−/−)/CaBP-D28k(−/−) mice, if the mice are viable.

Acknowledgments—We thank Y. Nakagawa for measuring serum and urinary salt concentrations, Y. Jiang for bone x-ray analysis, and W. Liu for assistance in bone histology.

REFERENCES

1. Bronner, F., and Pansu, D. (1999) *J. Nutr.* **129,** 9–12
2. Fullmer, C. S. (1992) *J. Nutr.* **122,** 644–650
3. Hoenderop, J. G., Willems, P. H., and Bindels, R. J. (2000) *Am. J. Physiol.* **278,** F352–F360
4. Hoenderop, J. G., van der Kemp, A. W., Hartog, A., van de Graaf, S. F., van Os, C. H., Willems, P. H., and Bindels, R. J. (1999) *J. Biol. Chem.* **274,** 8375–8378
5. Hoenderop, J. G., Dardenne, O., Van Abel, M., Van Der Kemp, A. W., Van Os, C. H., St-Arnaud, R., and Bindels, R. J. (2002) *FASEB J.* **16,** 1398–1406
6. Johnson, J. A., and Kumar, R. (1994) *Semin. Nephrol.* **14,** 119–128
7. Friedman, P. A., and Gesek, F. A. (1995) *Physiol. Rev.* **75,** 429–471
8. Christakos, S., Gabrielides, C., and Rhoten, W. B. (1989) *Endocr. Rev.* **10,** 3–26
9. Cao, L. P., Bolt, M. J., Wei, M., Sitrin, M. D., and Li, Y. C. (2002) *Arch. Biochem. Biophys.* **400,** 118–124
10. Li, Y. C., Bolt, M. J. G., Cao, L.-P., and Sitrin, M. D. (2001) *Am. J. Physiol.* **281,** E558–E564
11. Li, H., and Christakos, S. (1991) *Endocrinology* **128,** 2844–2852
12. Varghese, S., Lee, S., Huang, Y. C., and Christakos, S. (1988) *J. Biol. Chem.* **263,** 9776–9784
13. Varghese, S., Deaven, L. L., Huang, Y. C., Gill, R. K., Iacopino, A. M., and Christakos, S. (1989) *Mol. Endocrinol.* **3,** 495–502
14. Huang, Y., Lee, S., Stolz, R., Gabrielides, C., Pansini-Porta, A., Bruns, M. E., Bruns, D. E., Miffin, T. E., Pike, J. W., and Christakos, S. (1989) *J. Biol. Chem.* **264,** 17454–17461
15. Ferrari, S., Molinari, S., Battini, R., Cossu, G., and Lamon-Fava, S. (1992) *Exp. Cell Res.* **200,** 528–531
16. Gagnon, A., Simboli-Campbell, M., and Welsh, J. (1994) *Kidney Int.* **45,** 95–102
17. Airaksinen, M. S., Eilers, J., Garaschuk, O., Thoenen, H., Konnerth, A., and Meyer, M. (1997) *Proc. Natl. Acad. Sci. U. S. A.* **94,** 1488–1493
18. Li, Y. C., Pirro, A. E., Amling, M., Delling, G., Baron, R., Bronson, R., and Demay, M. B. (1997) *Proc. Natl. Acad. Sci. U. S. A.* **94,** 9831–9835
19. Li, Y. C., Amling, M., Pirro, A. E., Priemel, M., Meuse, J., Baron, R., Delling, G., and Demay, M. B. (1998) *Endocrinology* **139,** 4391–4396
20. Li, Y. C., Kong, J., Wei, M., Chen, Z. F., Liu, S. Q., and Cao, L. P. (2002) *J. Clin. Investig.* **110,** 229–238
21. Beamer, W. G., Donahue, L. R., Rosen, C. J., and Baylink, D. J. (1996) *Bone* **18,** 397–403
22. Feng, J. Q., Zhang, J., Dallas, S. L., Lu, Y., Chen, S., Tan, X., Owen, M., Harris, S. E., and MacDougall, M. (2002) *J. Bone Miner. Res.* **17,** 1822–1831
23. An, Y. H., and Martin, K. L. (2003) *Handbook of Histology Methods for Bone and Cartilage*, pp. 295–352, Humana Press, Totowa, NJ
24. Silver, J., Naveh-many, T., Mayer, H., Schmeizer, H. J., and Popovtzer, M. M. (1986) *J. Clin. Investig.* **78,** 1296–1301
25. Silver, J. (2001) *J. Clin. Investig.* **107,** 1079–1080
26. Hoenderop, J. G., Nilius, B., and Bindels, R. J. (2002) *Biochim. Biophys. Acta* **1600,** 6–11
27. Peng, J. B., and Hediger, M. A. (2002) *Curr. Opin. Nephrol. Hypertens.* **11,** 555–561
28. Breslau, N. A. (1996) in *Primer on Metabolic Bone Diseases and Disorders of Mineral Metabolism* (Favus, M. J., ed) 3rd Ed., pp. 49–57, J. B. Lippincott/Williams & Wilkins, Philadelphia
29. Bushinsky, D. A. (1999) in *Primer on Metabolic Bone Diseases and Disorders of Mineral Metabolism* (Favus, M. J., ed) 4th Ed., pp. 67–74, J. B. Lippincott/Williams & Wilkins, Philadelphia
30. Van Cromphaut, S. J., Dewerchin, M., Hoenderop, J. G., Stockmans, I., Van Herck, E., Kato, S., Bindels, R. J., Collen, D., Carmeliet, P., Bouillon, R., and Carmeliet, G. (2001) *Proc. Natl. Acad. Sci. U. S. A.* **98,** 13324–13329
31. Sooy, K., Kohut, J., and Christakos, S. (2000) *Curr. Opin. Nephrol. Hypertens.* **9,** 341–347
32. Lee, C. T., Huynh, V. M., Lai, L. W., and Lien, Y. H. (2002) *Kidney Int.* **62,** 2055–2061
33. Faucheux, C., Bareille, R., and Amedee, J. (1998) *Biochem. J.* **333,** 817–823
34. Bellido, T., Huening, M., Raval-Pandya, M., Manolagas, S. C., and Christakos, S. (2000) *J. Biol. Chem.* **275,** 26328–26332
35. Zeitz, U., Weber, K., Soegiarto, D. W., Wolf, E., Balling, R., and Erben, R. G. (2003) *FASEB J.* **17,** 509–511
36. Sooy, K., Schermerhorn, T., Noda, M., Surana, M., Rhoten, W. B., Meyer, M., Fleischer, N., Sharp, G. W., and Christakos, S. (1999) *J. Biol. Chem.* **274,** 34343–34349
37. Peng, J. B., Chen, X. Z., Berger, U. V., Vassilev, P. M., Tsukaguchi, H., Brown, E. M., and Hediger, M. A. (1999) *J. Biol. Chem.* **274,** 22739–22746
38. Weber, K., Erben, R. G., Rump, A., and Adamski, J. (2001) *Biochem. Biophys. Res. Commun.* **289,** 1287–1294
39. Song, Y., Peng, X., Porta, A., Takanaga, H., Peng, J. B., Hediger, M. A., Fleet, J. C., and Christakos, S. (2003) *Endocrinology* **144,** 3885–3894